CHEMICAL ENGINEERING TRANSACTIONS
VOL. 57, 2017
A publication of AIDIC
The Italian Association of Chemical Engineering
Online at www.aidic.it/cet
Guest Editors: Sauro Pierucci, Jiří Jaromír Klemeš, Laura Piazza, Serafim Bakalis

ISBN 978-88-95608- 48-8; **ISSN** 2283-9216
DOI: 10.3303/CET1757146

The Direct Hydrodeoxygenation of Vegetable Oil over Pt-Sn/Al_2O_3 Catalysts

Andrey V. Chistyakov[*a,b], Mark V. Tsodikov[a,b], Polina A. Zharova[a], Vladimir V. Kriventsov[c], Michele Corbetta[d], Flavio Manenti[d]

[a]Topchiev Institute of Petrochemical Synthesis RAS, Leninskii pr. 29, Moscow 119991, Russia
[b]Semenov Institute of Chemical Physics RAS, Kosygina str., 4, Moscow 119991, Russia
[c]Boreskov Institute of Catalysis, Siberian Branch of the Russian Academy of Sciences, pr. Lavrent'eva 5, Novosibirsk, 630090 Russia
[d]Politecnico di Milano, Dipartimento di Chimica, Materiali e Ingegneria Chimica "Giulio Natta", Piazza Leonardo da Vinci, 32, 20133 Milano, Italy
chistyakov@ips.ac.ru

The evolution of the structure of Pt–Sn/Al_2O_3 catalysts and their catalytic properties in the reaction of the reductive deoxygenation of rapeseed oil fatty acid triglycerides (FATGs) have been studied. It has been shown that the use of the heterometallic complex as a precursor with a tin to platinum molar ratio of 5 results in the formation of clusters of nanosized tin (2+; 4+) oxides and particles of a metastable $PtSn_{3\pm\delta}$ alloy on the surface of the catalyst after reductive activation. In the presence of this catalyst, the exhaustive conversion of the feed FATGs and the selectivity for hydrocarbons above 98% have been achieved. The gaseous products CO, CO_2, and CH_4 are formed in trace quantities. The results show that the deoxygenation occurs not via the known decarboxylation and decarbonylation route, but also through the step of the selective reduction of oxygen and almost complete suppression of cracking of the organic moieties of FATGs.

1. Introduction

One of the main feedstocks for the production of biofuels is fatty acid triglycerides produced from various oil-yielding crops and waste edible fats (Demirbas, 2008). The so called green diesel produced from vegetable oils by their of deoxygenation and isomerization is superior in the basic fuel parameters to the first generation biodiesel consisting of methyl esters of fatty acids, and to diesel fuel produced from petroleum. A high cetane number (CN=75–90), a lower pour point and a high oxidation stability are the advantages of green diesel (Holmgren et al., 2007). The first step in the process for producing third generation hydrocarbon feedstock from oils is deoxygenation. The catalytic deoxygenation occurs primarily as a result of decarbonylation and decarboxylation reactions, as well as varying degrees of cracking of formed hydrocarbon fragments of esters with the formation of C_1, C_2, and carbon oxides as byproducts (Kovacs et al., 2010). These reactions result in the loss of valuable carbon-containing mass and, consequently, in a decrease in the profitability of the deoxygenation process. Modification of the platinum alumina catalyst with tin is widely used to increase the selectivity and stability of the catalysts in the reforming process aimed to produce aromatic high-octane gasoline components, and in the reactions of isobutane and propane dehydrogenation (Iglesias et al., 2010). The main feature of the catalysts is the use of low concentrations of active components. A number of studies have shown that the addition of tin to a platinum-containing catalyst promotes the formation of tin oxides in an oxidizing atmosphere, and Pt–Sn alloy particles of different composition in a reducing one. The formation of a bimetallic Pt–Sn alloy results in a substantial decrease in the size of deposited particles in comparison with single-component systems (Liu et al., 2014), and makes it possible to significantly reduce the cracking activity of the catalyst, as well as to increase the stability of the catalyst with respect to the formation of condensation products on its surface (Mikulec et al., 2009).
In paper (Chistyakov et al., 2015) it was shown that a high selectivity for the reductive deoxygenation of rapeseed oil fatty acid triglycerides (FATGs) and microalgae oil extract is achieved in the presence of a

Please cite this article as: Chistyakov A., Tsodikov M., Zharova P., Kriventsov V., Corbetta M., Manenti F., 2017, The direct hydrodeoxygenation of vegetable oil over pt-sn/al2o3 catalysts, Chemical Engineering Transactions, 57, 871-876 DOI: 10.3303/CET1757146

catalyst comprising Pt–Sn/Al_2O_3, in which the bimetallic components are obtained by depositing them from a heterometallic complex containing a metal–metal (Pt–Sn) bond in its structure. The quantitative conversion of specific esters used as model compounds to hydrocarbon components is achieved at a tin to platinum molar ratio of 5:1. At this ratio of the active ingredients the reductive deoxygenation of FATGs also occurs selectively with a yield of C_3–C_{18} hydrocarbon fraction of 99%. In the presence of the catalyst the deoxygenation of an ester used as a model compound proceeds almost quantitatively with the formation of hydrocarbons, the number of carbon atoms in which corresponds to acyl moieties of the ester, and water (Tsodikov et al., 2015). In this regard, it is important to study the ratio of quantities of deposited active ingredients, as well as the influence of the precursor on the structure and selectivity of the catalyst in the deoxygenation of rapeseed oil FATGs, one of the main feedstocks for the production of diesel fuel components.

This paper presents the results of the study on the effect of the ratio of supported components, tin and platinum, on the evolution of the structure of the catalytically active sites and, accordingly, on the selectivity in the deoxygenation of FATGs.

2. Materials and Methods

The feedstock was rapeseed oil manufactured by the Russkie Semena company (fatty acid composition of the oil transesterified with methanol is given in (Tsodikov et al., 2015).

The conversion of rapeseed oil FATGs was studied on a PID Eng&Tech microcatalytic unit with a fixed bed flow reactor.

Gaseous reaction products were analyzed by the GC. Liquid organic products in the aqueous and organic phases were analyzed by gas GC–MS, using MSD 6973 (Agilent) and Automass%150 (Delsi Nermag).

The active components in different Pt:Sn molar ratios of 1, 3 and 5 were deposited on γ-Al_2O_3 by the impregnation method. The platinum loading on the catalysts was 0.4 wt.%. Single-metal precursors $(PPh_3)_2PtCl_2$ and $SnCl_2$, as well as the heterometallic Pt–Sn bond-containing complex precursor $(PPh_4)_3[Pt(SnCl_3)_5]$ obtained according to a unique procedure, were used as precursors for catalyst preparation of the (Shapovalov et al., 2014).

High-resolution transmission electron microscopy (HRTEM) (a JEOL JEM-2010 microscope with a grid resolution of 0.14 nm and an accelerating voltage of 200 kV), and energy-dispersive X-ray spectroscopy (EDS) (EDAX attachment to an EDAX microscope, X-ray microanalyzer with a semiconductor Si(Li) detector with a resolution of ~ 130 eV) were used to study the morphology, structure, composition, and particle size distribution of the samples of the synthesized Pt–Sn/Al2O3 catalysts after heat treatment, reductive activation, and catalysis. The size of the supported particles of the active ingredients was defined as the maximum linear dimension. To construct particle size distribution histograms, the data for 192–243 particles were statistically processed. Before testing, a 0.1 gram sample of the catalyst was placed in 30 mL of C2H5OH and sonicated for 300 s. A drop of the resulting mixture was placed on a copper grid coated with amorphous carbon, dried for 1 h, placed in the microscope and studied. The preparation for the measurements of the catalytic systems taken after reduction and catalysis was carried out in an inert argon atmosphere.

The HRTEM and EDS studies were carried out in accordance with the recommendations by the manufacturers of the microscope and accessories. The methodological aspects of the research are similar to those carried out previously for supported platinum catalysts (Beck et al., 2010).

The measurement of photoelectron spectra was conducted at room temperature on a Theta Probe spectrometer (ThermoFisher Scientific, UK) using Al Kα monochromatic radiation. The photoelectron spectra were recorded at constant absolute energy resolution with an increment of 0.1 eV. The measurements were carried out at a pressure in the analysis chamber of ~5·10–7 Pa. The analyzed spectra were approximated by Gaussian profiles or by their combination, and the background due to secondary electrons and photoelectrons that have lost energy, by a straight line. The spectrometer energy scale was calibrated by the standard method using the following values of binding energies: Cu $2p_{3/2}$, 932.7 eV; Ag $3d_{5/2}$, 368.3; eV, and Au $4f_{7/2}$, 84.0 eV (Nava et al., 2007).

3. Results and discussion

Table 1 shows the results on the yield of C_1 hydrocarbon products, which were the total gaseous products CH_4, CO and CO_2, and C_{18} (total alkanes and olefins) formed as a result of the reductive deoxygenation of FATGs on the catalysts containing different proportions of the active components. From the table it is seen that monometallic Pt/Al_2O_3 catalyst at 420°C is not selective in the formation of C_{18}. In its presence the hydrocracking and decarboxylation processes occur, whereby the reaction products contain 64% of heptadecane and 14-22% of C_2-C_{16} alkanes (Tsodikov et al., 2015). Monometallic Sn/Al_2O_3 catalyst is active only at an elevated temperature of 480°C, resulting in the formation of mainly C_3-C_{12} alkane-olefin

hydrocarbons (80%) which are the products of hydrocracking, and aromatics (14%) which are the products of dehydrocyclization.

Table 1. Yield of the main products of rapeseed oil conversion in the presence of mono- and bimetallic Pt and Sn catalysts.

Temperature,°C	Ratio of active ingredients Sn : Pt	1:1	3:1	5:1 separate applying	5:1	Pt	Sn
	product yield, wt %						
400	C_{18}	44.85	68.7	66.5	83.87		
	C_1	3.69	0.4	3.2	0.05		
420	C_{18}	32	48.6		76.1	14.89	
	C_1	3.65	1.8		0.3	3.44	
480	C_{18}	7.6	44.8		37.2		
	C_1	7	1.1		0.24		0.2

Bimetallic Pt and Sn-containing systems exhibit a high selectivity in the reductive deoxygenation of FATGs. Thus, from Table 1 it is seen that the increase in the tin to platinum molar ratio from 1 to 3 upon their deposition on the alumina surface from a mixture of the individual precursors, at 400°C substantially increases the selectivity of the reductive deoxygenation with the formation of C_{18} up to 68.7% and almost negligible contribution of the decarboxylation reaction. A further increase in the active ingredients (tin to platinum) molar ratio to 5 upon their deposition on the support from a mixture of the individual complexes does not lead to a change in selectivity.

A different result was obtained upon the deposition on the Al_2O_3 surface of the heterometallic complex, in which the active ingredients are linked by chemical metal-metal bond. In the presence of this catalyst the C_{18} content reaches 84%, with traces of methane and carbon oxides. The selectivity in the formation of C_{18} hydrocarbons relative to the content of the acyl moiety in the starting ester reaches 90% at a total selectivity for C_3–C_{18} hydrocarbons of more than 98%. By increasing the reaction temperature up to 480°C the yield of C_{18} is decreased with a slight increase in the yield of gaseous products. Hydrocracking with the formation of an intermediate C_3–C_{15} fraction becomes the dominant reaction (Chistyakov et al., 2015). However, despite increased hydrocracking of the organic moieties of FATGs the catalyst obtained from the heterometallic complex exhibits a higher selectivity in the reductive deoxygenation.

TEM of a sample with a tin to platinum molar ratio of 1, after its heat treatment showed that the sample is composed of Al_2O_3 decorated with Pt and Sn particles. For the gamma-modification of alumina, agglomerates with particle size from 100 nm to 1 μm and a crystallite size of ~ 10‑30 nm are typical. Note that the platinum-containing active ingredient is highly dispersed, its content is very low, and in most photographs taken at high resolution only the carrier is present. According to the EDS data, the content of the applied ingredient is known to be below 1%, since the signals corresponding to Pt and Sn are only slightly higher than the background level. At a high resolution, high contrast areas can be detected; the areas can be divided into two different types: fine particles of ~ 3‑4 nm in size (indicated by a circle), and clusters with a size of ~ 0.5 nm. Rather, the small particles are those of Pt. The individual particles or reflexes typical of Sn were not detected. Perhaps, tin ions interact strongly with the carrier surface oxygen.

TEM of a system, in which the molar ratio of deposited tin to platinum is 3 showed that the morphology of the active ingredient of the sample almost does not differ from the previous one (highly dispersed, the content is very small, at most of the high-resolution images only the carrier is present). Just as in the previous sample, Pt presumably is present as clusters with a size of less than 0.5 nm, and small particles of ~ 3 nm in size. The individual particles of Sn were not detected as well. Particle of ~ 3 nm in size were detected, which is metallic Pt according to the EDS data. The picture for the sample prepared by using precursors with a Sn:Pt ratio of 5, is not much different from that of the system in which the ratio of the active ingredients was 3.

For the samples obtained from the heterometallic complex at a Sn:Pt ratio of 5 the EDX data show that the quantity of Sn is higher in comparison with other samples and is close to ~1 at % compared to Al. Particles of Pt, as in the previous samples, are present in the form of clusters and small particles (marked with red circles) (Fig. 1). After reductive activation, in contrast to the original sample with a Sn:Pt ratio of 1, two types of platinum nanoparticles are present on the support surface: (1) there are platinum metal nanoparticles supported on Al_2O_3, the particle size is of an order of several (~ 2) nm; and (2) nanoparticles (~ 3‑5 nm) on the Al_2O_3 support surface were detected, which may include $PtSn_{3\pm\delta}$ metastable compound, according to the EDS data.

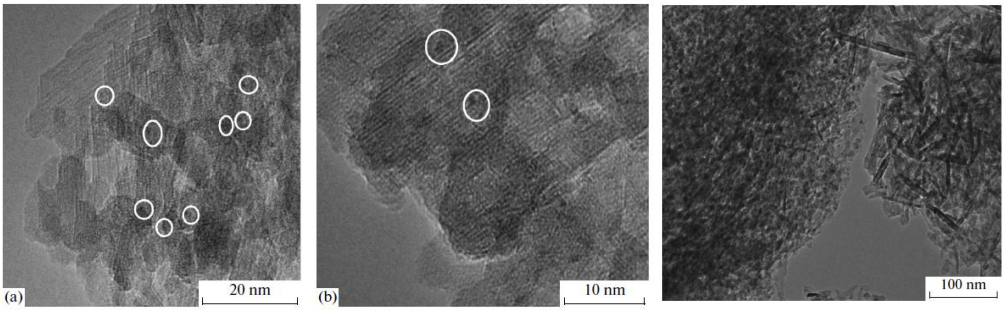

Figure 1. TEM photomicrographs at different magnifications of a sample of the catalyst 1Pt-5Sn, obtained from the heterometallic complex (a, b). And this sample after the catalysis.

The samples containing the active ingredients (Sn:Pt = 3 and 5) and produced by the separate deposition of $(PPh_3)_2PtCl_2$ and $SnCl_2$, do not differ morphologically from the sample with Sn:Pt = 1 reduced after the reaction. Amorphous carbon is present on the agglomerates of carrier particles with a crystallite size of ~ 10‑25 nm (Fig. 1). According to the EDS data, the content of Pt and Sn is also very low, less than 1% (in the survey spectra the signals are only slightly higher than the background level; an accurate assessment is difficult because of a large error in the background subtraction), however, there are areas of increased concentration.

The sample with a Sn:Pt ratio of 5 obtained by applying the heterometallic complex contains only two types of nanoparticles: Pt nanoparticles with a size of 1‑2 nm, and ones with dimensions of ~ 3‑5 nm and of $PtSn_{3\pm\delta}$ composition, according to the EDS data. Note that the individual nanoparticles of "pure" tin were not found, as well as in the previous samples).

This sample was morphologically nearly identical to the previous samples reduced after the reaction (Sn:Pt = 1, and Sn:Pt = 3). Similarly, the carrier, the γ-Al_2O_3 modification, consists of agglomerates with particle size from 100 nm to 1 μm, and a crystallite size of ~ 10‑25 nm. Amorphous carbon is present on the carrier surface. According to the EDS data, the quantity of Sn is higher in comparison with other samples, but is close to ~ 1 at.% compared to Al; the Pt content is very low, less than 1%. After the reduction and catalysis, the micrographs show a similar pattern‑there are two kinds of particles: reduced Pt particles 1‑2 nm in size, and ones 4‑5 nm in size. Nanoparticles of individual tin were not found.

Table 2 lists the results of the quantitative analysis of the surface of the samples studied by XPS: (1) the source sample with the ratio of active catalyst ingredients Sn/Pt=5, (2) the catalyst after the reductive activation, and (3) after catalysis. The table also shows the results of the analysis of the initial carrier, tin catalyst, and heterometallic $(PPh_4)_3[Pt(SnCl_3)_5]$ precursor. The Sn:Pt ratio in the catalysts differs considerably from the ratio in the heterometallic precursor, which may be caused by features of the application and a nonuniform distribution of the metal-containing ingredients on the catalyst surface. In comparison with the precursor the surface of 1 is enriched in tin, and that of 2 and 3 is depleted.

The presented data show that the metal complex precursor contains a large quantity of carbon, the concentration of which substantially exceeds the concentration of carbon on the carrier surface. This may indicate an incomplete removal of carbon in the preparation of the catalysts, which apparently hinders the complete oxidation of the metals. The analysis of C 1s spectrum of the precursor has shown that 6% of C atoms are in the oxidized state in the form of C–OH/C–O–C groups, and the remaining 94%, in the form of C–C and C–H.

Note that taking into account the surface charge according to the registered Al 2s peak, the binding energy of the C–C, I state in the C 1s spectrum of the Sn/Al_2O_3 sample is 283.7 eV, which is by 1.1 eV lower than the widely used in practice value of 284.8 eV (Naumkin et al., 2012). In this case, the electron binding energies of the $Sn3d_{5/2}$ sublevel for the Sn/Al_2O_3 and $PtSnO_x$ samples also differ by 1.1 eV, indicating a change in the interaction of carbon with the carrier in the presence of tin. When selecting the C 1s peak binding energy of 284.8 eV as the reference point, we get nearly the same binding energies of the Sn3d5/2 electrons for the Sn/Al_2O_3 and $PtSnO_x$ samples, which indicates the same chemical states of the tin atoms in both samples. This result suggests that the Pt in the source PtSnOx sample does not affect the oxidation state of the tin atoms, and indicates the existence of Pt–O–Sn bonds in the precursor.

The Pt $4f_{7/2}$ electron binding energy of 72.9 eV is in the range 72.4–74.6 eV typical of PtO (Naumkin et al., 2012), and the corresponding electron binding energy for $Sn3d_{5/2}$ (1) that makes 487.0 eV is close to 486.8 eV measured for SnO_2 (Larchev et al., 1984). With regard to the second state with an electron binding energy of 488.0 eV, it, to our knowledge, has no analogs in the literature and should therefore be attributed to differential

charging; in this case, it is due to the difference in the interaction of metal atoms with impurity carbon and the carrier, as indicated by the difference in the C1s–Al2s energy interval (Table 3). An increase in the binding energy and peak broadening, as well as an increase in the surface core level shift reflects the size effects of platinum and tin particles (Ramstad et al., 1999).

Table 2. Results of quantitative analysis by XPS

	Al, at.%	O, at.%	C, at.%	Pt, at.%	Sn, at.%	Cl, at.%	P, at.%	Pt/Sn
Support	35.09	59.97	4.94					
1	25.49	45.16	24.68	0.11	2.32	2.25		0.05
2	25.04	46.11	28.26	0.12	0.47			0.26
3	25.82	47.64	26.02	0.11	0.40			0.28
Sn/Al_2O_3	31.63	51.11	16.91		0.34			
Precursor		10.58	70.87	0.65	3.7	9.19	4.98	0.16

Table 3. Binding energies of photoelectron peaks and the energy intervals between them.

	$Pt_{4f7/2}$	$Sn_{3d5/2}$	$Sn_{3d5/2}$	C_{1s}	C_{1s}- $Pt_{4f7/2}$	$Sn_{3d5/2}$ (1)- C_{1s}	$Sn_{3d5/2}$ (2) –C_{1s}	$Sn_{3d5/2}$ (1)- $Pt_{4f7/2}$	C_{1s}- Al_{2s}
1	72.3	485.9	487	284.8	212.5	201.1	202.2	413.6	165.8
2	71.6	486.2	487.3	284.8	213.2	201.4	202.5	414.5	165.1
3	71.8	486.3	487.4	284.8	213	201.5	202.6	414.4	165.1
Sn/Al_2O_3	–	487	488.1	284.8	-	202.2	203.3	-	164.7
$PtSnO_x$	72.9	487	488	284.8	211.9	202.2	203.2	414	-
Al_2O_3	-	-	-	284.8	-	-	-	-	165.8

From the comparison of the binding energies for $Pt4f_{7/2}$ electrons with the literature data (Nava et al., 2007) it follows that after the heat treatment of the deposited complex (sample 1) the platinum is in the form of metal particles and is probably partially oxidized.

For the Sn 3d spectra of the catalysts, regardless of the method of accounting for the surface charge, a decrease in the binding energy of the electrons as compared to the single-component Sn/Al_2O_3 and the precursor is typical, which is likely to be related to the transition of a part of the tin to a lower oxidation state, caused by a change in the interaction with the Pt during the catalyst formation. Comparison of the Auger parameters calculated from the initial spectra with published data also indicates the Sn^{2+} state in the catalysts and in the single-component Sn/Al_2O_3, in contrast to the precursor, for which the Sn^{4+} state is typical.

After the reductive activation a decrease in the $Pt_{4f7/2}$ binding energy in the catalysts indicates a decrease in the level of interaction with oxygen and the formation of Pt–Sn alloy particles. This is also indicated by changes in the Sn $3d_{5/2}$ (1)–Pt $4f_{7/2}$ energy interval relative to the precursor.

The breakdown of the Sn_{3d} spectra into the components showed that in the reduced samples a decrease occurs in the binding energy of the low-energy state which depends on the Sn : Pt ratio and the binding energy of Pt $4f_{7/2}$ sublayer electrons. The consideration of the set of the data obtained, namely, electron binding energies for Sn $3d_{5/2}$ and Pt $4f_{7/2}$, along with their difference, and the relevant data for the Pt-Sn/MgO system (Llorca et al., 1999), points to the possible existence of Sn–Pt bonds. Taking into account the concentrations of the elements and the presence of differential charging, the O–Sn(C)–Pt form would be more precise. Comparison of the Pt $4f_{7/2}$ peak widths with the corresponding values in the spectrum of the foil indicates the manifestation in the spectra of the dimensional effect caused by the small size of the Pt particles, which is in agreement with the TEM data, from which it follows that the size of the platinum clusters is less than 2 nm, and the size of the alloy particles is 3–5 nm.

The results allow us to conclude that in the activated state the active ingredients consisting of superfine Pt, Sn^{2+}, Sn^{4+} particles and particles of $PtSn_{3\pm\delta}$ alloy are present on the surface of the catalyst system. Such a high selectivity of the catalyst in the reductive deoxygenation of esters resulting in the quantitative yield of hydrocarbon fragments and water is probably caused by the chemisorption of the oxygen atoms of the carbonyl and ether groups on the ions of tin (2^+–4^+).

The route of the ester oxygen reduction may include the participation of intermetallic $PtSn_{3\pm\delta}$ clusters. The cracking activity of such clusters, is, probably, substantially decreased compared to platinum-containing centers of the reforming catalysts. A decrease in the cracking activity of the catalyst comprising finely divided particles of the Pt–Sn alloy is pointed out in the reaction of isobutane to butane dehydrogenation, wherein at a high reaction temperature light C_1–C_3 hydrocarbons almost were not generated (Nava et al., 2007). Metallic Pt

clusters with a high degree of dispersion (not more than 1.5–2 nm) are, probably, covered (encapsulated) by carbon preventing their agglomeration and substantially lowering the activity in the cracking and decarboxylation reactions. Using the heterometallic complex comprising a metal-metal bond between the platinum and the tin atoms, along with an increase in the Sn : Pt molar ratio, increases the concentration on the carrier surface of the active ingredients, intermetallic clusters likely arranged closely to the particles of tin oxide that are likely may be centers of nucleophilic coordination of oxygen atoms of esters. Almost complete absence of carbon oxides and light hydrocarbon cracking products, and the formation of alkanes and alkenes with the same number of carbon atoms as in the ester acyl groups accounts for a high selectivity of the deoxygenation process in the presence of the catalyst comprising the highly dispersed bimetallic active ingredients.

4. Conclusions

Thus, in the presence of the Pt-Sn/Al_2O_3 catalyst prepared by applying the heterometallic complex, highly selective reductive deoxygenation of FATGs is achieved, resulting in the formation of only alkane-alkene hydrocarbons that are the hydrocarbon fragments of FATGs; C_1 byproducts formed as a result of cracking reactions and the removal of carbonyl and carboxyl groups of esters are nearly absent. A high selectivity of the catalyst in the reaction of the reductive decomposition of esters is provided by two important factors: particle size factor and the structure of the precursor of the active ingredients. A small size of tin oxide and intermetallic alloy clusters probably set conditions for their interaction only with ester oxygen atoms as the most active centers of the substrate, but the clusters are spatially hindered for the reaction with unsaturated bonds in the carbon chain of the acyl moieties. The heterometallic complex used as a precursor of the active ingredients comprises a direct bond between the platinum and the tin atoms, which probably favors the formation on the surface of adjoining tin-containing and intermetallic centers having the ability for chemisorption of FATGs by oxygen atoms, and for its reduction with hydrogen, and a weakened ability for cracking hydrocarbon fragments. The results do not allow us to estimate the sequence or concerted action of the deoxygenation reaction. To this end, we will conduct the theoretical analysis of the energy and activation parameters of the reactions.

Acknowledgments

This study was financially supported by Russian Scientific Foundation Grant No. 15-13-30034.

References

Beck I.E., Kriventsov V.V., Ivanov D.P., Yakimchuk E.P., Novgorodov B.N., Zaikovskii V.I., Bukhtiyarov V.I., 2010, Journal of Structural Chemistry, 51, 11-19.

Chistyakov A.V., Zharova P.A., Tsodikov M.V., M. V., Shapovalov S.S., Pasinskiy A. A., Murzin V.Y., Moiseev I. I., 2015, Doklady Chemistry, 460, 26-28.

Demirbas A., 2008, Biodiesel: A Realistic Fuel Alternative for Diesel Engines, Springer, London.

Holmgren J., Gosling C., Marinangeli R., Marker T., Faraci G., Perego C., 2007, UOP Report AM-07-11.

Iglesias-Juez A., Beale A. M., Maaijen K., Weng T. C., Glatzel P., Weckhuysen B. M., 2010, Journal of Catalysis, 276, 268-279.

Kovacs S., Boda L., Leveles L., Thernesz A., Hancsók J., 2010, Chemical Engineering Transactions, 21, 1321.

Larchev V. and Popova S., 1984, Inorganic Materials. 20, 693-695.

Liu X., Lang W.Z., Long L.L., Hu C.L., Chu L.F., Guo Y., 2014, Chemical Engineering Journal, 247, 183-192.

Llorca J., Homs N., Leon J., Sales J., Fierro J.L.G., De La Piscina P.R., 1999, Applied Catalysis A, 189, 77-86.

Mikulec J., Cvengros J., Jorikova L., Banic M., Kleinová A., 2009, Chemical Engineering Transactions, 18, 475-480.

Naumkin A.V., Kraut-Vass A., Gaarenstroom S.W., Powell C.J., 2012, *NIST X-ray Photoelectron Spectroscopy Database. Version 4.1* ,Gaithersburg, http://srdata.nist.gov/xps/.

Nava N., Angel P., Salmones J., Baggio-Saitovitch E., Santiago P., 2007, Applied Surface Science, 253, 9215-9220.

Ramstad A., Strisland F., Raaen S., WorrenT., Borg A., Berg C., 1999, Surface Science, 425, 57-67.

Shapovalov S.S., Pasynskii A.A., Torubaev Yu.V., Skabitskii I. V., Scheer M., Bodensteiner M., 2014, Russian Journal of Coordination Chemistry, 40, 131-137.

Tsodikov M.V., Chistyakov A.V., Gubanov M.A., et al., 2015, Izv. Akad. Nauk, Ser. Khim., 9, 2062-2068.